Field measurement and modeling of near-bed sediment transport processes with fluid mud layer in Tokyo Bay

Yasuyuki Nakagawa · Kazuo Nadaoka · Hiroshi Yagi · Ryuichi Ariji · Haruo Yoneyama · Kazuhiro Shirai

Abstract Tokyo Bay is one of the estuaries in Japan with a high population of almost 26 million people in the basin area. One of the major concerns for the environment in this water area is the decreasing ecosystem functions including the deterioration of water and sediment qualities caused by various anthropogenic activities. Since the bottom sediments around almost the entire area of the inner bay consist of fine materials with a high organic content, which cause the deterioration of water quality through processes such as hypoxia, an understanding of the fine sediment dynamics in the Bay is crucial for an environmental assessment of the water area. This paper proposes a model for the key processes of fine sediment dynamics, which reflects field data about muddy bed structures and their dynamics obtained during the monitoring campaign in 2007. One of the specific features of the sediment in the Bay at present is the persistent existence of fluid mud layers (water content over 300 %) with a thickness of around a few decimeters, which might be caused by deposition of abundant organic particles due to eutrophication. The present study shows that diffusion flux model delivers quite reliable results for estimating erosion flux from the top of fluid mud layers after calibrating the model parameter against the time series data of vertical flux measured by an acoustic Doppler velocimeter system. This study also derives analytical solutions, based on the Bingham fluid concept, of advection flux in the fluid mud layer on which external shear stress force is applied.

Keywords Fluid mud · Erosion flux · Resuspension · Bingham fluid model · Tokyo Bay

1 Introduction

An understanding of the distribution and transport processes of muddy sediment, which consists of silt and clay fractions, is crucial for predicting and evaluating the environmental evolution of water systems in estuarine and coastal areas.

Y. Nakagawa (✉) · R. Ariji
Port and Airport Research Institute,
3-1-1 Nagase,
Yokosuka 239-0826, Japan
e-mail: y_nakagawa@ipc.pari.go.jp
URL: www.pari.go.jp

K. Nadaoka
Tokyo Institute of Technology,
2-12-1 O-okayama, Meguro-ku,
Tokyo 152-8550, Japan

H. Yagi
National Research Institute of Fisheries Engineering,
7620-7 Hasaki,
Kamisu, Ibaraki 314-0408, Japan

H. Yoneyama · K. Shirai
Yokohama Port and Airport Technical Research Office,
Ministry of Land, Infrastructure, Transport and Tourism,
2-1-4 Hashimoto-cho, Kanagawa-ku,
Yokohama 221-0053, Japan

Present Address:
R. Ariji
Tokyo Airport Construction Office, Ministry of Land,
Infrastructure, Transport and Tourism,
3-1-1 Haneda-kuko, Ohta-ku, Tokyo 144-0041, Japan

Present Address:
H. Yoneyama · K. Shirai
Port and Airport Research Institute,
3-1-1 Nagase, Yokosuka 239-0826, Japan

Regarding the processes by which organic and inorganic substances are exchanged between the muddy sediment and water column, several sophisticated models have been developed and used to evaluate the ecosystem through the changes in water quality (e.g., Sohma et al. 2008; Nobre et al. 2010). However, the effects of the transport processes of muddy bottom sediment are not incorporated in most water quality and ecosystem models, even though the dynamic transport processes of sediments greatly affect the surrounding water environment. Since one of the reasons for this omission is a limited knowledge of sediment dynamics, especially of intermittent events, it is desirable to capture and analyze such events as storm-driven resuspension and sediment discharge during flood conditions. This can be accomplished by making long-term measurements in the field (e.g., Traykovski et al. 2007).

Tokyo Bay is one of the estuaries in Japan. The Bay has a high population of almost 26 million people in the basin area. One of the major concerns for the environment in the Bay area is the deterioration of water and sediment qualities having a negative impact on benthic organisms (e.g., Kodama and Horiguchi 2010). The site of the present study is beyond the mouth of the Tama River, which discharges into the west coast of the inner Bay. A monitoring project has been running at this site since 2006 in order to grasp the environmental evolution of physical, chemical, and ecological aspects. The present authors have taken part in a study on the sedimentary processes and carried out analyses of sediment core samples to gather information on sediment properties and to monitor changes in sediment characteristics in the area (Ariji et al. 2011; Nakagawa et al. 2011). Through preliminary studies, we have shown that the key to modeling the sediment dynamics at the site is the prediction of mud bed transport with high water content, i.e., the fluid mud layer.

Many researchers have constructed models of fluid mud dynamics, some of which have been applied to estuaries (e.g., Odd and Cooper 1989) and continental shelves (e.g., Harris et al. 2005). However, since the properties and dynamics of fluid mud are highly site-dependent, a universal model does not work for fluid mud dynamics.

Therefore, this study examines numerical formulations to estimate the sediment transport rate near the sea bed, as preliminary numerical modeling for simulating the entire sediment transport dynamics in Tokyo Bay in the future. The study focuses on estimating the erosion flux from the fluid mud layer and the horizontal flux in the mud layer, considering the muddy sediment characteristics observed in Tokyo Bay. For the erosion flux model, a diffusion flux type of equation is calibrated through a comparison with field measurements of resuspension process of muddy sediments. We also derive analytical solutions of the velocity profile in the fluid mud layer using the Bingham model, which makes it possible to estimate sediment mass flux in the fluid mud layer under the effect of shear stress.

2 Study site

2.1 Overview of study site

This study focused on the mouth of the Tama River, which is in the northwestern part of inner Tokyo Bay, Japan (Fig. 1). The Bay has a surface area of 992 km^2 with an average depth of around 19 m, and a semi-diurnal, meso-tidal condition with a maximum spring tidal range of less than 2 m. Several rivers flow into the upper part of the Bay with a total drainage basin area of 7,600 km^2. The Tama River has the second largest basin (1,240 km^2) and carries around 20 m^3/s at typical background flow rates and over 1,000 m^3/s during flood events. The coastal area including the mouth of the Tama River region is highly industrialized. Furthermore, a newly extended runway of Tokyo International Airport is located near the mouth of the river.

2.2 Topography and sediment characteristics

The topography of the target site is characterized as a delta front formed by the Tama River. An acoustic image obtained by a subbottom profiler (Edgetech, SB-242) from the topset (river side) of the delta through the bottomset (offshore side) is shown in Fig. 2. Sand is dominant in the topset and inside the river basin, and the offshore regions from the foreset to the bottomset are dominated by very soft mud. The muddy sediments are more than 99 % silt and clay with a high water content of around 300 % or thin fluid mud layers, and so acoustic images near the bottom layers are relatively fuzzy.
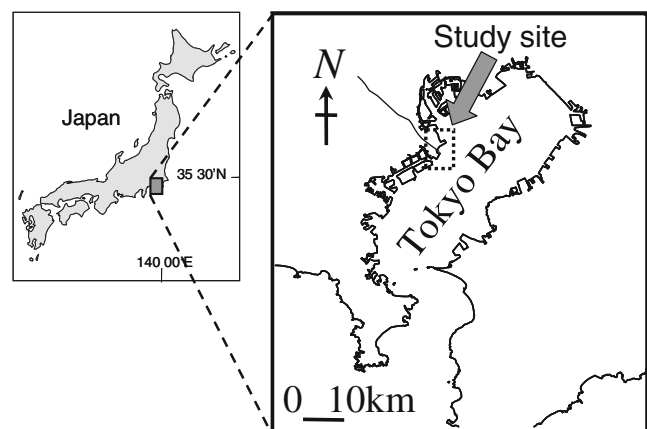
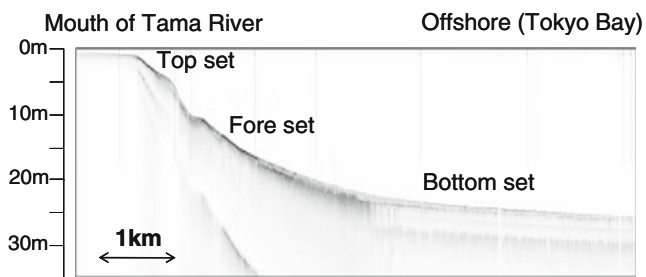Fig. 1 Location of Tokyo Bay and the Tama River

Fig. 2 Topography at the mouth of the Tama River

The water content is defined as the ratio of the weight of water to the weight of solids in a sample. Typical profiles of water content measured for sediment cores taken at monitoring points in the study site are shown in Fig. 3. Water content in the near-surface layer in offshore areas such as Stn. B and C is over 400 %, showing the existence of thin fluid mud layers that cover the underlying consolidated mud (Fig. 4). Observed data show loose muddy sediment covering a broad area around the inner Bay. Since the bottom sediments around almost the entire area of the inner bay consist of fine materials, modeling of the sediment transport dynamics including the fluid mud layer is considered to be crucial for evaluating the water environment of the site.

3 Field observation and data analysis

3.1 In situ measurements

Long-term measurements were also conducted around the site with moored and bottom-mounted sensors to determine the dynamics of the bottom and suspended sediment transport processes. The monitoring campaign in the summer of 2007 covered a storm event with high waves followed by extensive flooding through the Tama River due to the pas-

sage of a typhoon. The near-bottom data set, including information about currents and turbidity, was obtained at the offshore site of Stn. B by using several acoustic and optical sensors as shown in Fig. 5. A Nortek Vector Acoustic Doppler Velocimeter (ADV) measured three-dimensional velocities at 10 cm above the bottom every half hour at 8 Hz in about 2-min bursts (1,024 data per burst). Optical backscatter sensors (OBS; Compact-CLW, JFE Advantech Co.) were moored at several levels near the bottom to measure suspended sediment concentration (SSC) profiles. Measured optical backscatter intensity was calibrated using sediment samples taken from the site to the SSC in units of milligrams per liter.

3.2 Field data analysis

3.2.1 Estimation of bed shear stresses

Bed shear stress was calculated with a bottom boundary model by Soulsby (1997) in this study. Mean current ($U = (u^2 + v^2)^{1/2}$) and representative wave velocity (u_b) were calculated from the ADV measurements of three-dimensional velocity at 10 cm above the bottom. The mean current stress is expressed by

$$\tau_c = \rho_w C_f U^2 \tag{1}$$

where ρ_w is water density. The friction factor for mean current, C_f, is set at 0.0041 referenced to the measurement height (=0.1 m) above the bed. Wave stress is given by

$$\tau_w = \frac{1}{2} \rho_w f_w u_b^2 \tag{2}$$

with the following wave friction factor, f_w (Soulsby 1997)

$$f_w = 1.39 (A/z_0)^{-0.52} \tag{3}$$

Fig. 3 Monitoring site locations and water content profiles of core samples taken from the monitoring sites ("contour" represents the water depth in the map for sampling locations)
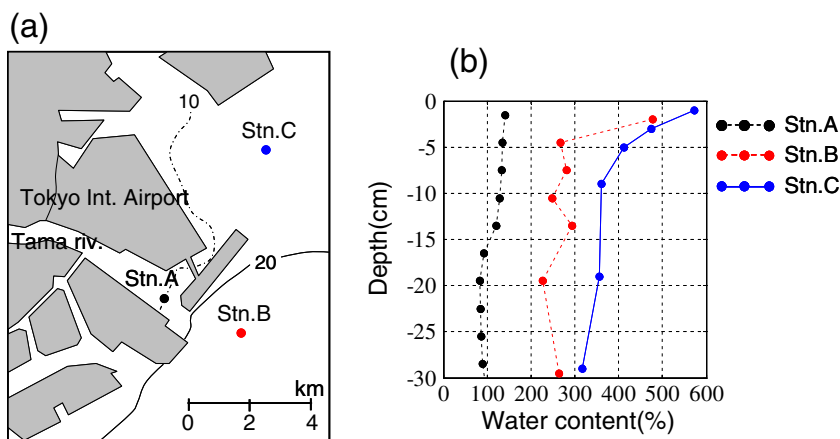
Fig. 4 Fluid mud on surface layer

where the wave orbital amplitude $A = u_b T / 2\pi$ and T is the wave period. The bottom roughness length, z_0, is assumed to be 0.2 mm as proposed by Soulsby (1997) for muddy bed environment. The value of the wave friction factor f_w varied between 0.003 and 0.05 in the present analysis. The representative wave velocity, u_b, is defined as (Traykovski et al. 2007)

$$u_b = \sqrt{2(u_{w\_rms}^2 + v_{w\_rms}^2)} \tag{4}$$

where the root mean square velocities were calculated with wave band variation of the ADV data over frequencies from 0.03 to 0.25 Hz. The nonlinear combined wave–current stress was calculated by the following equations as the maximum stress, τ_{max}, and the mean stress, τ_m (Soulsby 1997)

$$\tau_{max} = \left[(\tau_m + \tau_w \cos\phi)^2 + (\tau_w \sin\phi)^2 \right]^{0.5} \tag{5}$$

$$\tau_m = \tau_c \left[1 + 1.2 \left(\frac{\tau_w}{\tau_c + \tau_w} \right)^{3.2} \right] \tag{6}$$

where ϕ is the angle between the mean current and dominant wave direction.
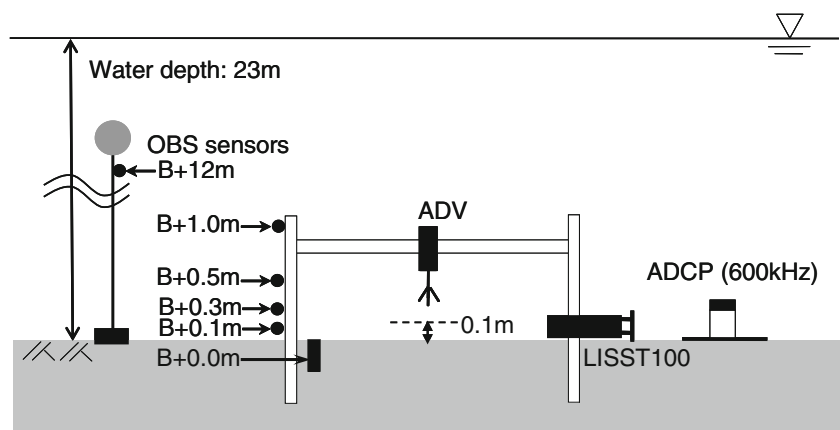
3.2.2 Erosion flux and bed elevation measurements

The ADV system can be used to estimate the suspended sediment concentration using the acoustic backscatter signal (e.g., Hay and Sheng 1992; Kawanishi and Yokoshi 1997; Fugate and Friedrichs 2002). In the present study, backscatter intensity was calibrated with SSC data obtained by the OBS at the same elevation in the vicinity of the ADV sensor. The relationship between the measured SSC and the mean acoustic backscatter intensity per burst is shown in Fig. 6. Based on the correlation, acoustic backscatter measured by the ADV was calibrated to the SSC. The backscatter data of the ADV were recorded at the same sampling rate as the velocity measurement with the frequency of 8 Hz during each 2-min burst every 30 min. The data can be used to estimate the vertical turbulent diffusion of suspended sediment as the Reynolds flux

$$F_z = \overline{c'w'} \tag{7}$$

where c' and w' represent fluctuating components of the suspended sediment concentration and the vertical velocity measured by the ADV, respectively. These fluctuations are defined as the deviation from the mean- and waveband variations. In Section 5 of this paper, temporal variation of the flux is used to validate the proposed formulation to estimate the resuspension flux.

Acoustic devices were used to measure bed elevation in several previous works (e.g., Andersen et al. 2006; Verney et al. 2007); acoustic backscatter records obtained by the ADV were used for this purpose in the present study. The instrument receives and records the backscatter signal not only from the velocity measurement range but also from other surrounding ranges (Nortek 2004) as shown in Fig. 7. The distance from the sensor to the bottom boundary can be clearly detected in the profile of the backscatter data.

3.3 Observed data in the storm and flood event

While the instrument was deployed from August to September 2007, Tokyo Bay experienced an extreme storm and

Fig. 5 Instrumentation layout for bottom boundary measurement
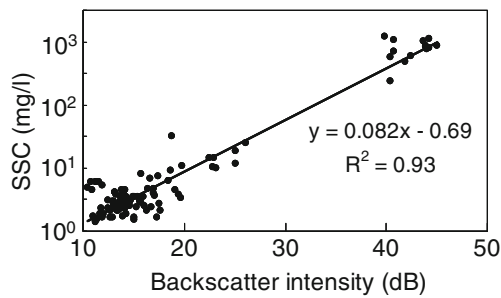
Fig. 6 Comparison of suspended sediment concentration estimated OBS with ADV backscatter

flood event due to the passage of a typhoon in early September. With strong southeasterly winds reaching 25 m/s, the significant wave height exceeded 2.5 m, and the wave period was over 5 s at the time of closest passage of the typhoon (Fig. 8a, d, e). According to statistics based on the long-term wave records from 1983 to 1992 at a monitoring station in the Bay (Japan Weather Association 1994), the recurrence probability of the wave event is less than 1 %, and the waves were the highest in the last 10 years.

Coinciding with the wave event, there was also a prominent discharge of fresh water from the Tama River, peaking at over 3,500 m^3/s (Fig. 8b) and recording the largest flood since 1982. The wind data were measured by the Automated Meteorological Data Acquisition System at the Haneda station, operated by the Japanese Meteorological Agency. The wave gauge is located at the Tokyo Bay Light House station (35°33′58″N, 139°49′41″E) near Stn. C in Fig. 3 where the water depth is about 14 m, some 6 km north from Stn. B.

Temporal variations of SSC, turbulent diffusion flux, and bed level are shown in Fig. 9 compared with the force condition during the extreme storm and flood event between September 5 and 12. During the period of high shear stress caused by waves and currents on September 7, the near-bed SSC rapidly increased with a high concentration of 2,000 mg/l just
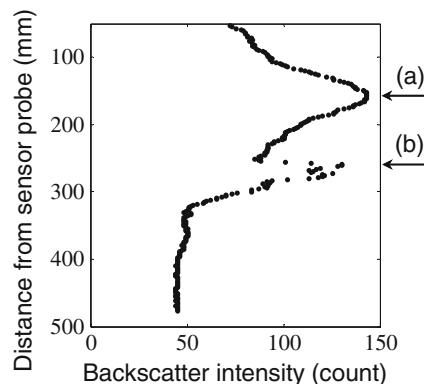
Fig. 7 Typical example of backscatter intensity profile obtained by the ADV measurement with **a** echo from velocity measurement layer and **b** echo from the bottom

above the bottom (B+0.0 m), 1,000 mg/l at 10 cm, and 100 mg/l at 50 cm. During the high near-bed SSC event, the turbulent diffusion flux of sediments calculated by Eq. (7) also showed higher values in the upward direction during the period. At the same time, the sea floor underwent slight erosion of 20 mm according to acoustic measurements of the bed elevation.

The data show a deposition of 50 mm following the erosion event, where the combined shear stress decreased to 0.3 Pa. During this deposition period, the SSC at the lowest layer, B+0.0 m, experienced an extremely high concentration of over 30,000 mg/l indicating the existence of fluid mud near the bed. In spite of the continuous deposition during the period, the SSC at B+0.0 m decreased, which was probably due to the limitation of the sensor range.

4 Estimation of near-bed sediment fluxes

The sediment concentration or density profile is characterized as shown in Fig. 10, considering the observed near-bed structures around the study site. There is a clear gap between the sea water and the top of the thin fluid mud layer over the consolidated mud. Key processes that should be estimated to model this muddy sediment environment include vertical transport rate expressed as upward flux (F_{up}) and downward flux (F_{down}). It is also necessary to model the advection process of the sediment in the mud layer in horizontal directions. This paper examines methods of estimating these processes.

4.1 Vertical fluxes

The settling flux, based on the simultaneous erosion and deposition concept (e.g., Winterwerp and van Kesteren 2004), is given by:

$$F_{down} = w_s C_b \qquad (8)$$

where w_s is the settling velocity of the suspended sediment and C_b is the concentration. For the upward flux in the water column, the following diffusion flux formulation (e.g., Ross and Mehata 1989) can be applied:

$$F_{up} = -K_z \frac{\partial C}{\partial z} \qquad (9)$$

where K_z is diffusivity, which can be modeled using the gradient Richardson number, R_i, and the diffusivity in the neutral condition without stratification, K_0:

$$K_z = K_0 (1 + \beta R_i)^{-\alpha}. \qquad (10)$$

The parameters α and β in the equation are set at 3.33 and 1.5, respectively, as proposed by Munk and Andersen

Fig. 8 Time series of **a** wind, **b** fresh water discharge of Tama River, **c** tide, and **d** significant wave height and **e** period
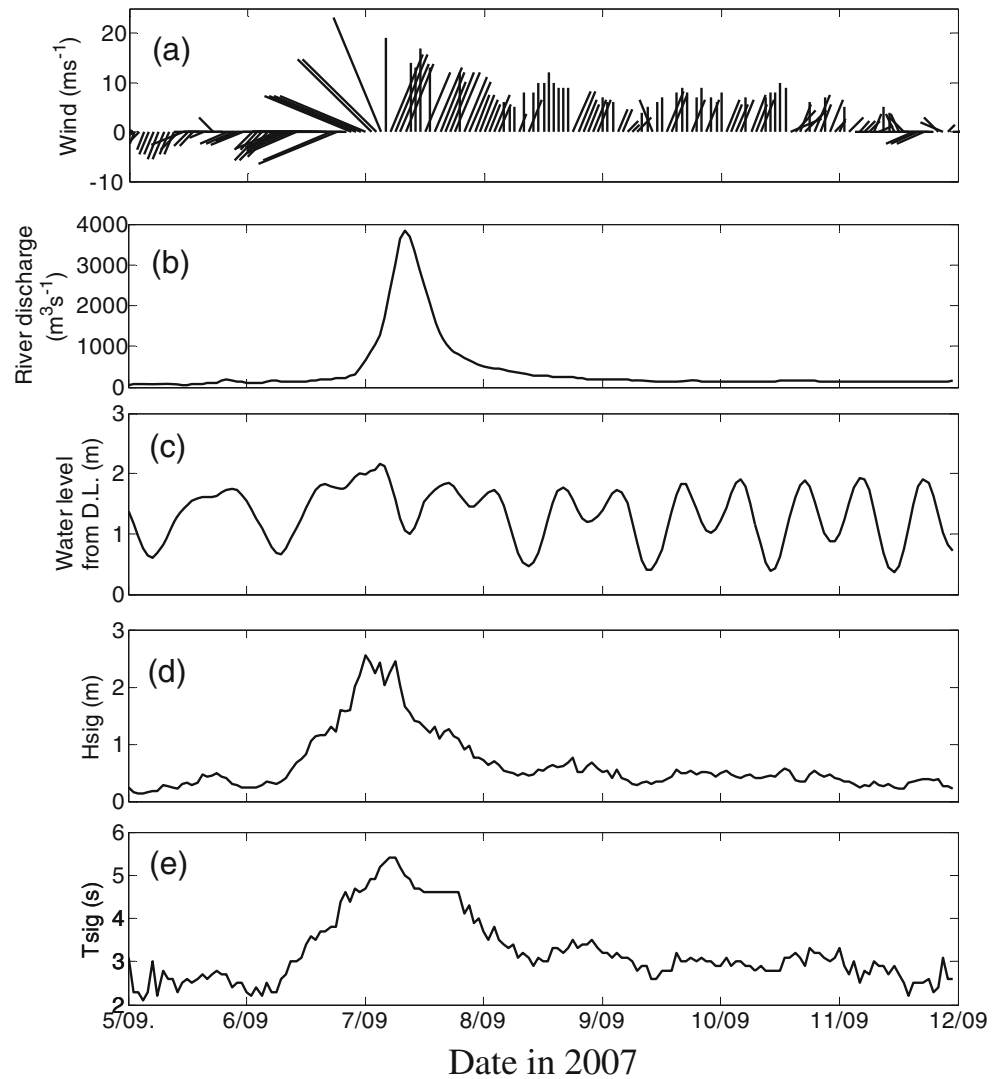
(1948). The gradient Richardson number, R_i, is the ratio of potential to kinetic energy gradients and is expressed in the following form,

$$R_i = -\frac{g}{\rho} \frac{(\partial \rho / \partial z)}{(\partial u / \partial z)^2} \tag{11}$$

where g is the acceleration due to gravity, ρ is the local fluid bulk density, and u is the current speed in the horizontal direction. The bulk density is related to the sediment concentration, C, in the fluid as:

$$\rho = \rho_w + C[(\rho_s - \rho_w)/\rho_s] \tag{12}$$

where ρ_w is the density of water and ρ_s is the density of sediment particles.

In the present study, Eq. (9) was used to estimate the upward flux between the fluid mud layer and the upper water column. The estimation was carried out for the observed forcing and suspended sediment conditions during the storm event as described in Section 3.2.

4.2 Fluid mud flow

For estimating the advection flux in the fluid mud layer, an analytical solution for the velocity profile in the mud layer was derived by assuming non-Newtonian fluid behavior in the layer. Many previous works dealt with mud flow as a non-Newtonian fluid (e.g., Liu and Mei 1989; Huang and Garcia 1999; Knoch and Malcherek 2011). Here, the Bingham fluid model is used in which the relationship between stress and strain is expressed as:

$$\tau = \tau_y \mathrm{sgn} \frac{\partial u_m}{\partial z} + \mu \frac{\partial u_m}{\partial z}, \quad \text{if } |\tau| \geq \tau_y \tag{13.a}$$

$$\mu \frac{\partial \mu_m}{\partial z} = 0, \quad \text{if } |\tau| < \tau_y \tag{13.b}$$

where μ is the kinematic viscosity and τ_y the yield stress of the fluid mud. These parameters depend on the bulk density and mineralogy. Analytical solutions for the vertical profiles

Fig. 9 Observed data during storm and flood event of **a** bottom shear stresses, **b** SSC, **c** erosion flux, and **d** bed elevation change
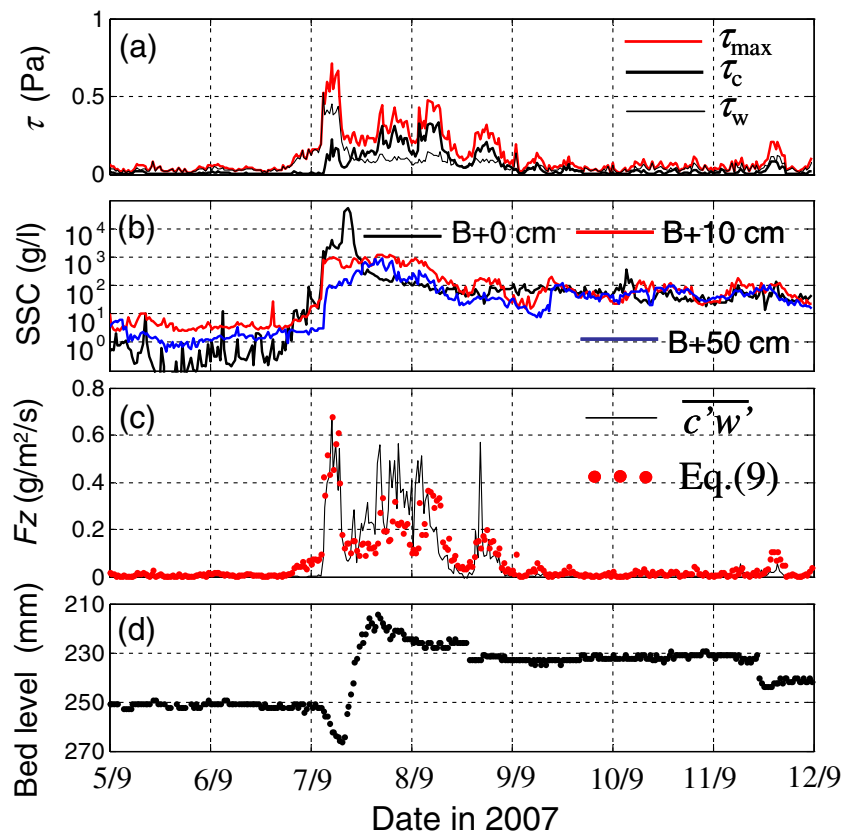
of the horizontal current speed, u_m, in the fluid mud layer are derived from an integral form of Eq. (13):

$$u_m(z) = \frac{1}{\mu} \int_{-h_y}^{z} \left[\tau(z) - \tau_y(z) \right] dz \qquad (14)$$

The lower limit of the integration interval, $-h_y$, is the yield surface level at which the external force, $\tau(z)$, is equal to the yield shear stress, $\tau_y(z)$, in the mud layer. The shear stress distribution in the mud layer can be derived from momentum balance equations.
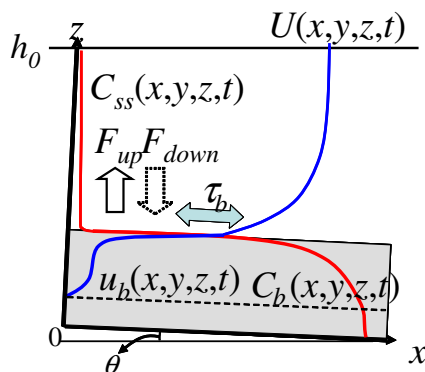
Fig. 10 Schematic diagram of the transport process of mud bed with thin fluid mud layer

Under a simplified condition with a flat bed and equilibrium state in space and time, external shear stress in the mud layer becomes a constant, τ_b. The external stress represents the shear stress at the boundary between the upper water column and the mud layer. On the other hand, non-uniformity of yield shear stress in the mud layer is taken into account in the present analysis. The distribution profile was determined by considering the observed density profiles in the mud layers as described precisely in Section 5.

5 Results

5.1 Erosion flux estimation

The erosion flux during the observed storm period was estimated with Eq. (9) by using the field measurements of forcing and suspended sediment conditions described in Section 3.2. For calculating the diffusivity in Eq. (10), the modified Richardson number R_i' is introduced:

$$R_i' = -\frac{g \Delta h (\rho_{10} - \rho_b)}{\tau_{b\_max}} \qquad (15)$$

where Δh is the distance between the bottom and the ADV measurement point (10 cm), ρ_{10} is the bulk density of sea
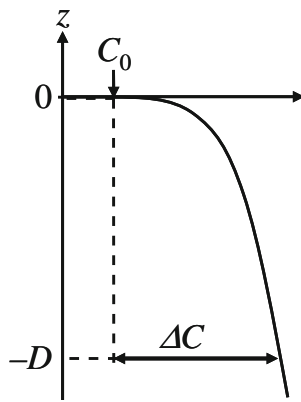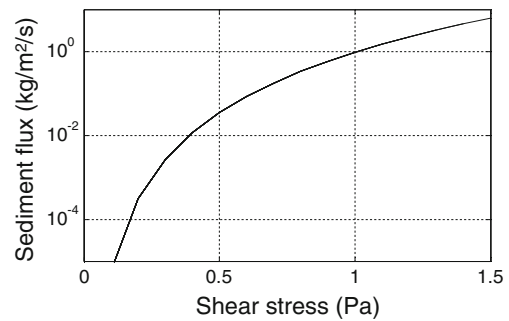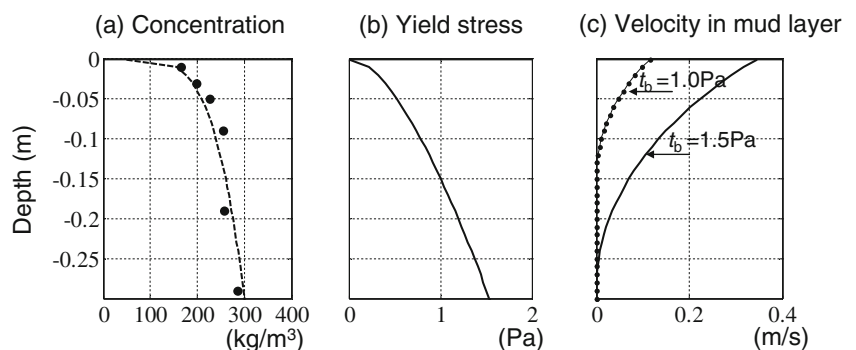
Fig. 11 Definition of parameters for sediment concentration profile

Fig. 13 Calculated sediment flux in mud layer under shear stress by overlying water current

water with suspended sediment at 10 cm above the bed, and ρ_b is that at the surface of the fluid mud layer. The bottom shear stress, τ_{b_max}, is evaluated by the velocity measurement data as non-linear combined wave–current stress as described in Section 3.2.

By substituting Eq. (15) into Eq. (10), the vertical flux was calculated with Eq. (9) for the period of the storm event in September 2007 shown in Fig. 9. The results estimated by Eq. (9) are plotted in Fig. 9c compared with the directly measured resuspension flux calculated as Reynolds flux. The estimation delivers quite reliable results, except the slight overestimates of resuspension during the early period of the storm event around September 7. This can be improved in practice by introducing a critical R_i' for erosion. This result implies that Eq. (9) is applicable to the bottom boundary condition of the resuspension flux in the case of an unconsolidated loose muddy bottom.

For the estimation by Eq. (9), the parameter K_0 is calibrated and set at a constant value of 0.0044 m²/s for the result in Fig. 9, considering the time series of the directly measured flux or Reynolds flux by Eq. (7). Note that the modified Richardson number R_i' [Eq. (15)] is not the same as the expression of flux Richardson number; non-dimensional friction factors for current and waves

are included in the bottom shear stress term in Eq. (15). Therefore, the calibrated value of the parameter K_0 above is not equivalent to the diffusivity in the neutral condition. However, it is remarkable that the diffusive flux expression dependent on the Richardson number and vertical gradient of the mean concentration can reliably reproduce the temporal variation of the measured Reynolds flux after the adequate calibration of the coefficient.

5.2 Derivation of fluid mud flux formula

Considering the observed near-bed structure of the muddy sediments, we propose a method for estimating horizontal sediment transport flux in the mud layer. By integrating Eq. (14), we can obtain a vertical velocity profile in the fluid mud layer. In order to make the integration of Eq. (14) possible, we introduce the following relationship between the yield shear stress, τ_y, and the sediment concentration, C_m, proposed by van Kessel and Kranenburg (1996),

$$\tau_y(z) = c_1 \left[\frac{C_m(z)}{\rho_s} \right]^{c_2} \tag{16}$$

where the non-dimensional empirical parameters c_1 and c_2 are set at 1,000 and 3, respectively, and ρ_s represents the density of sediment particles (=2.6 g/cm³). For the sediment

Fig. 12 Profiles of modeled sediment properties: **a** concentration, **b** yield shear stress, and **c** estimated current speed in mud layer (C_0=50 kg/m³, ΔC=250 kg/m³, D=0.3 m, μ=0.47 Pas)

concentration profile of $C_m(z)$, the following function (e.g., Foda et al. 1993) is introduced:

$$C_m(z) = C_0 + \Delta C(-z/D)^{0.25} \tag{17}$$

In Eq. (17), C_0 is the concentration at the top of the fluid mud layer, and ΔC represents an increase in the concentration at the depth of $-D$ from the surface of the mud layer as shown in Fig. 11. These parameters are chosen so that the approximate function, Eq. (17), closely fits the field data of sediment concentrations as shown in Fig. 12a. Substituting the distribution function of the yield shear stress, Eq. (16), into Eq. (14) allows us to derive a formulation of the velocity profile in the mud layer under the shear stress on the surface of the mud layer, τ_b, as

$$u_m(z) = \frac{1}{\mu} \left[(\tau_b - \alpha_0)(z + h_y) + \alpha_0 \alpha_1 \frac{4}{5} D \left(\frac{(-z)^{5/4} - h_y^{5/4}}{D^{5/4}} \right) \right.$$
$$\left. + \alpha_0 \alpha_2 \frac{2}{3} D \left(\frac{(-z)^{3/2} - h_y^{3/2}}{D^{3/2}} \right) + \alpha_0 \alpha_3 \frac{4}{7} D \left(\frac{(-z)^{7/4} - h_y^{7/4}}{D^{7/4}} \right) \right]$$
$$\tag{18}$$

where

$$\alpha_0 = c_1 \left(\frac{C_0}{\rho_s} \right)^3, \alpha_1 = 3 \frac{\Delta C}{C_0}, \alpha_2 = 3 \left(\frac{\Delta C}{C_0} \right)^2, \alpha_3 = \left(\frac{\Delta C}{C_0} \right)^3.$$

The height of the yield surface, h_y, is defined by the relations between external shear stress and internal yield shear stress. The results of computing velocity profiles using Eq. (18) are indicated in Fig. 12c in the two cases of $\tau_b = 1.0$ and 1.5 Pa, as examples. The parameters in the model used in the present study are indicated in the figure. In both shear stress cases, the shear flows appear at the near surface of the mud layer under the effect of the shear stress exerted by the current of the upper water layer. The mobility layers are limited up to the yield surface level.

Furthermore, by considering the velocity profile in the fluid mud layer and the fitted concentration profile, the horizontal sediment transport rate can be formulated as

$$\mathbf{q}_m(x,y,z,t) = \int_{-h_y}^{h_b(x,y,t)} C_m(x,y,z,t) \mathbf{u}_m(x,y,z,t) dz$$
$$= \frac{D^2}{\mu} \left[(\tau_b - \alpha_0) \left(\frac{1}{2} C_0 h_y'^2 + \frac{16}{45} \Delta C h_y'^{\frac{9}{4}} \right) - \alpha_0 \alpha_1 \left(\frac{4}{9} C_0 h_y'^{\frac{9}{4}} + \frac{8}{25} \Delta C h_y'^{\frac{5}{2}} \right) \right]$$
$$+ \frac{D^2}{\mu} \left[-\alpha_0 \alpha_2 \left(\frac{2}{5} C_0 h_y'^{\frac{5}{2}} + \frac{16}{55} \Delta C h_y'^{\frac{11}{4}} \right) - \alpha_0 \alpha_3 \left(\frac{4}{11} C_0 h_y'^{\frac{11}{4}} + \frac{4}{15} \Delta C h_y'^3 \right) \right]$$
$$\tag{19}$$

where

$$h_y' = \frac{h_y}{D} = \left(\frac{C_0}{\Delta C} \right)^4 \left\{ \left(\frac{\tau_b}{c_1} \right)^{1/3} \frac{\rho_s}{C_0} - 1 \right\} \tag{20}$$

By using the above equation, horizontal sediment mass transport rate in the fluid mud layer can be estimated as a function of the external force or the bottom shear stress on the surface of the mud layer (Fig. 13). After appropriate validations of the results, the method could be applied for spatial mud transport simulations.

6 Conclusions

The present study examined the transport characteristics of a mud bed with a thin fluid mud layer observed in Tokyo Bay, where muddy sediments with high water content appear at the bed surface. Field measurements captured a near-bed process with erosion and deposition of the muddy sediments

during a storm and flood event. As a preliminary work for modeling the entire muddy sediment transport process in Tokyo Bay, estimation methods were examined for the key processes.

A diffusion flux model was calibrated and used for estimating the temporal variation of the vertical flux of resuspended sediment near the bed. For the calibration, field measurements of current and suspended sediment concentrations during a storm and flood event in Tokyo Bay were used. The estimated result showed reliable performance, implying that the diffusion flux type of formula can be applied for the bottom boundary condition of the erosion flux from an unconsolidated loose muddy bed.

The study also examined an estimation of total horizontal transport rate in the mud layer driven by external shear stress. Flow velocity profiles in the mud layer were derived from a set of basic equations, where the fluid mud layer was assumed to be a Bingham fluid. We also considered the observed vertical structure of the sediments in the study site and incorporated a distribution function, which fits the

sediment concentration profile, in the model. Analytical solutions for flow velocity in the fluid mud layer were derived under an arbitrary shear stress condition assuming an equilibrium state in space and time. The total advection flux in the mud layer can be estimated as a function of external force by the proposed model.

For the estimated horizontal sediment flux, there are no available data for validating the dynamics in the fluid mud layer. Therefore, the result is confined to a derivation of the analytical formula in this paper; the method remains to be validated appropriately in the future. Mathematically, the proposed methods in the present study could be easily applied for mud transport simulations by coupling with 3D hydrodynamic models.

References

Andersen TJ, Pejrup M, Nielsen AA (2006) Long-term and high-resolution measurements of bed level changes in a temperate, microtidal coastal lagoon. Mar Geol 226:115–125

Ariji R, Yagi H, Nadaoka K, Nakagawa Y, Ogawa H, Shimosako K, Shirai K (2011) Temporal and spatial variations of bottom sediment characteristics around the Tama River mouth in Tokyo Bay, Japan. The 21st International Offshore (Ocean) and Polar Engineering Conference, June 22, 2011

Foda MA, Hunt JR, Chou H-T (1993) A nonlinear model for the fluidization of marine mud by waves. J Geogr Res 98(C4):7039–7047

Fugate DC, Friedrichs CT (2002) Determining concentration and fall velocity of estuarine particle populations using ADV, OBS and LISST. Cont Shelf Res 22:1867–1886

Harris CK, Traykovski PA, Geyer ER (2005) Flood dispersal and deposition by near-bed gravitational sediment flows and oceanographic transport: a numerical modeling study of the Eel River Shelf, northern California. J Geophys Res 110:C09025. doi:10.1029/2004JC002727

Hay AE, Sheng J (1992) Vertical profiles of suspended sand concentration and size from multifrequency acoustic backscatter. J Geophys Res 97(C10):15,661–15,677

Huang X, Garcia MH (1999) Modeling of non-hydroplaning mudflows on continental slopes. Mar Geol 154:131–142

Japan Weather Association (1994) Bulletin of Meteorological and Oceanographic Condition in Tokyo Bay, Japan Weather Association, Tokyo, p. 420 (in Japanese)

Kawanishi K, Yokoshi S (1997) Characteristics of suspended sediment and turbulence in a tidal boundary layer. Cont Shelf Res 17(8):859–875

Knoch D, Malcherek A (2011) A numerical model for simulation of fluid mud with different rheological behaviors. Ocean Dyn 61:245–256

Kodama K, Horiguchi T (2010) Effects of hypoxia on benthic organisms in Tokyo Bay, Japan: a review. Mar Pollut Bull 63:215–220

Liu KF, Mei CC (1989) Spreading of thin sheet of fluid mud on an incline. J Coast Res 5:139–149

Munk W, Andersen ER (1948) Notes on a theory of the thermocline. J Mar Res 7(3):276–295

Nakagawa Y, Ariji R, Nadaoka K, Yagi H, Shimosako K, Shirai K (2011) Field measurement of erosion and deposition processes of muddy bed sediment during storm event in Tokyo Bay. Proc. of Coastal Sediments, ASCE, pp. 2403–2414

Nobre AM, Ferreira JG, Nunes JP, Yan X, Bricker S, Corner R, Groom S, Gu H, Hawkins AJS, Hutson R, Lan D, Lencart e Silva JD, Pascoe P, Telfer T, Zhang X, Zhu M (2010) Assessment of coastal management options by means of multilayered ecosystem models. Estuar Coast Shelf Sci 87:43–62

Nortek (2004) Vector current meter user manual. Nortek AS, Rud, p 84

Odd NVM, Cooper AJ (1989) A two-dimensional model of the movement of fluid mud in a high energy turbid estuary. J Coast Res 5:185–193

Ross MA, Mehata AJ (1989) On the mechanics of lutoclines and fluid mud. J Coast Res 5:51–61

Sohma A, Sekiguchi Y, Kuwae T, Nakamura Y (2008) A benthic-pelagic coupled ecosystem model to estimate the hypoxic estuary including tidal flat—model description and validation of seasonal/daily dynamics. Ecol Model 215:10–39

Soulsby RL (1997) Dynamics of marine sands. Thomas Telford Publications, London, p 249

Traykovski P, Wiberg PL, Geyer WR (2007) Observations and modeling of wave-supported sediment gravity flows on the Po prodelta and comparison to prior observations from the Eel shelf. Cont Shelf Res 27:375–399

van Kessel T, Kranenburg C (1996) Gravity current of fluid mud on sloping bed. J Hydraul Eng 122(12):710–717

Verney R, Deloffre J, Brun-Cottan J-C, Lafite R (2007) The effect of wave-induced turbulence on intertidal mudflats: impact of boat traffic and wind. Cont Shelf Res 27:594–612

Winterwerp JC, van Kesteren W (2004) Introduction to the physics of cohesive sediment in the marine environment. Elsevier, Amsterdam, p 466